JMEPEG (2001) 10:344–348 ©ASM International

Analyses of Effects of Temperature and Loading Rate on Fracture Toughness of High-Strength Low-Alloy Steels

L.C. Jian, L.S. Hua, and W.Y. Qing

(Submitted 29 March 2000)

A formula is derived for determining the influence of temperature and loading rate on dynamic fracture toughness of a high-strength low-alloy steel (HQ785C) from thermal activation analysis of the experimental results of three-point bend specimens as well as by introducing an Arrhenius formula. It is shown that the results obtained by the given formula are in good agreement with the experimental ones in the thermal activation region. The present method is also valuable to describe the relationship between dynamic fracture toughness and temperature and loading rate of other high-strength low-alloy steels.

Keywords fracture mechanism, fracture toughness, high-strength steel, temperature, thermal activation analysis

1. Introduction

It has been well known that, among the factors affecting material fracture characteristics, temperature and strain rate are two very important external ones. Most brittle fracture accidents with low stress occurred in steel structures due to low temperature and dynamic loading condition. The mechanism of plastic deformation and fracture of materials may change at different temperatures and strain rates.[1] At present, it has been widely investigated that the dynamic yield strength of steels varies with temperature and strain rate.[2] However, the research of dynamic fracture toughness of steels is mostly concentrated on the study of the influence of temperature under some loading conditions. Therefore, it is essential to systematically study the combined effects of temperature and loading rate on dynamic fracture toughness of steels in ensuring the safety application of their structural parts.

2. Experimental Details

The material tested was a special high-strength low-alloy steel designated as HQ785C in the Chinese steel standard, the chemical composition of which is listed in Table 1. The steel plate was received as quenched and tempered in the form of 20 mm thickness plate, with its microstructure being tempered martensite (Fig. 1). Its mechanical properties are given in Table 2.

Three-point bend specimens and instrumented impact specimens were machined from the plate according to GB4161-84 and GB2650-89 (Chinese National Standards, which are similar to ASTM E399-91 and ASTM E636-83, respectively), respectively.[3] The dimension of the three-point bend specimens is 130 mm × 28 mm × 14 mm, as shown in Fig. 2. The instrumented impact specimens are 55 mm in length, 10 mm in width and thickness, and 5 mm in crack length. Each of the specimens was fatigue precracked on a servohydraulic Material Testing System (MTS) according to the specifications of GB4161-84. The fatigue precracking frequency was 92 Hz. During the test, ethyl alcohol and liquid nitrogen were used to adjust the required temperatures below ambient for the experiment and an autoheating device was used to control the temperature over ambient.

Fracture toughness evaluation tests were carried out at a series of temperatures ranging from 77 to 333 K by an MTS-880 materials testing machine with crosshead speed of 0.01 and 50 mm/s and by a TINIUS-T84 instrumented impact machine with an impact speed of 5540 mm/s. When the load-point displacement rates, Δ, were 0.01 and 0.7 mm/s, a *X-Y* coordinate recorder was applied to record the P-Δ (load-loading point displacement) curve. When the rates were 50 and 5540 mm/s, a computerized data acquisition processing system was used.

The K_{Id} values in the lower-shelf region were determined according to the method of GB4161-84 by Eq 1; in the ductile-to-brittle transition and upper-shelf regions, J_{Id}, the critical J integral values were measured based on the relation, Eq 2, given by Rice *et al.*[4]

$$K_{Id} = \frac{P_Q S}{BW^{3/2}} Y\left(\frac{a}{W}\right) \quad \text{(Eq 1)}$$

$$J_{Id} = \frac{2U}{B(W - a)} \quad \text{(Eq 2)}$$

$$Y\left(\frac{a}{W}\right) = \frac{3\left(\frac{a}{W}\right)^{1/2}\left[1.99 - \left(\frac{a}{W}\right)\left(1 - \frac{a}{W}\right) \times \left(2.15 - 3.93\left(\frac{a}{W}\right) + 2.7\left(\frac{a}{W}\right)^2\right)\right]}{2\left(1 + \frac{2a}{W}\right)\left(1 - \frac{a}{W}\right)^{3/2}}$$

where B is the specimen thickness, W is the specimen width,

L.C. Jian, L.S. Hua, and **W.Y. Qing,** Central Iron and Steel Research Institute, No. 76 Xueyuan Nanlu, Haidian District, Beijing 100081, Republic of China. Contact e-mail: weldingli@263.net.

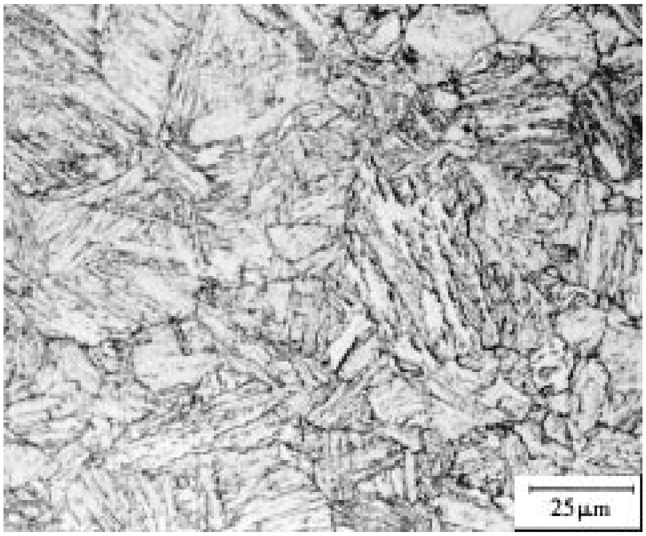

Fig. 1 Microstructure of tested materials

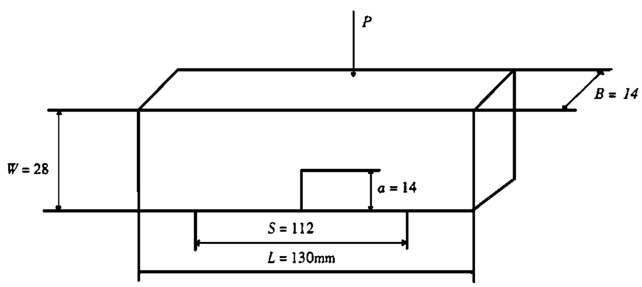

Fig. 2 The dimensions of a three-point bend specimen

Table 1 The chemical composition (wt.%)

C	Si	Mn	P	S	Cr	Mo	V	Cu	B
0.12	0.29	1.05	0.017	0.013	0.92	0.38	0.05	0.24	0.0015

Table 2 Mechanical properties (as-received)

			A_{KV} (J)	
σ_{ys} (MPa)	σ_{ult} (MPa)	ε_{ult} (%)	(253 K)	(233 K)
735	785	18	49, 66, 53	31, 28, 27

a is the crack depth, S is the span, U is the area under the load-loading point displacement curve until the crack extension point, and P_Q is the load as determined in GB4161-84.

In instrumented impact tests, J_{Id} values were measured over all temperature ranges, but the term U in Eq 2 was replaced by the area under the load-deflection curve up to the maximum load because detection of the crack extension point was difficult.

The value of J_{Id} was then converted into K_{Id} by the following equation:

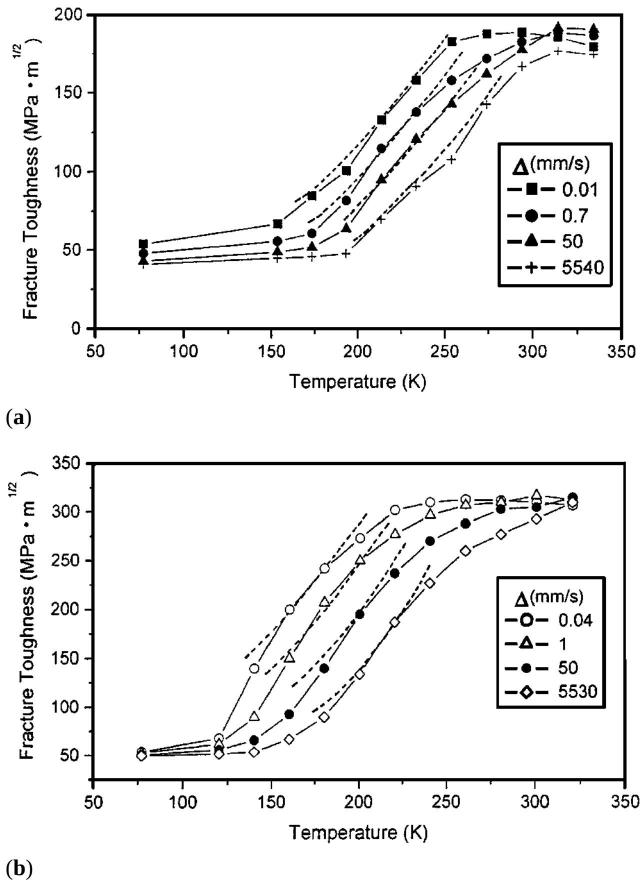

Fig. 3 Result of experimental K_{Id} values (the values calculated are shown in the dotted lines): (**a**) HQ785C steel and (**b**) 13Ni3CrMoV steel

$$K_{Id} = [EJ_{Id}/(1 - v^2)]^{1/2} \quad \text{(Eq 3)}$$

where E is the Young's modulus and v is Poisson's ratio.

3. Experimental Results and Thermal Activation Analysis

The curves in Fig. 3(a) show the experimental dynamic fracture toughness, K_{Id}, of HQ785C steel versus temperature at different loading rates. From Fig. 3(a), it can be shown that, when temperatures are over 253 K for $\dot{\Delta} = 0.01$ mm/s and 273 K for $\dot{\Delta} = 0.7$ mm/s, K_{Id} values have little dependence on temperature, *i.e.*, values are on the upper-shelf region. With the decrease of temperature or increase of loading rate, K_{Id} values are usually reduced. When the temperature is lowered to a certain critical temperature at some loading rate, approximately 153 K for $\dot{\Delta} = 0.01$ mm/s and about 213 K for $\dot{\Delta} = 5540$ mm/s, K_{Id} values will not be reduced with the decease of temperature, *i.e.*, the lower-shelf region has been reached.

It has been widely shown that the plastic flow of materials is governed by the thermally activated motion of dislocations and the relation between dynamic yield strength and temperature and strain rate, which agrees with the Arrhenius equation within some range of temperature and strain rate.[5] In fact, judging from the essence, fracture is the final result of materials deformation to a certain degree, with dislocations continually moving, gathering, and piling up under the action of external forces. Dynamic fracture toughness gives expression to the ability of materials to resist fracture and mainly depends on their ability to deform prior to fracture. Therefore, it is reasonable to assume that a materials dynamic fracture toughness parameter, such as K_{Id}, will also be controlled by the thermally activated motion of dislocations within certain ranges of temperatures and strain rates. According to the Arrhenius equation,[6]

$$\dot{\varepsilon} = \dot{\varepsilon}_0 \exp\left(-\Delta G_f/kT\right) \qquad \text{(Eq 4)}$$

where Δ G_f is the activation energy; $\dot{\varepsilon}_o$ is a frequency factor; k is Boltzmann's constant (k = 8.6112 mm $\times$ 10^{-5} ev/k); T is temperature in Kelvin; and $\dot{\varepsilon}$ is strain rate relative to l, r, t, and Δ and can be calculated by the following formula:[7]

$$\dot{\varepsilon} = \frac{r \cdot \dot{\Delta}}{t \cdot l} \qquad \text{(Eq 5)}$$

where r is the radius of the slip band with the specimen being bent, t is the slip bandwidth, l is the span (the distance between specimen supports), and $\dot{\Delta}$ is the loading-point displacement rate. Substituting Eq 5 into Eq 4, one can obtain

$$\dot{\Delta} = \frac{t \cdot l}{r}\,\dot{\varepsilon}_0 \exp\left(-\Delta G_f/kT\right) = X \exp\left(-\Delta G_f/kT\right) \qquad \text{(Eq 6)}$$

where $X = \frac{t \cdot l}{r}\,\dot{\varepsilon}_0$

Taking the logarithm for Eq 6, then Eq 6 may be rewritten in the following form:

$$\ln \dot{\Delta} = \ln X - \frac{\Delta G_f}{k} \cdot \frac{1}{T} \qquad \text{(Eq 7)}$$

Equation 7 can be plotted in the $ln\ \dot{\Delta}$-$1/T$ coordinate by the data from Fig. 3(a) at constant K_{Id} levels (Fig. 4a). With the same K_{Id} values, the relation between $ln\ \dot{\Delta}$ and T^{-1} is basically linear. Furthermore, the lines are approximately parallel at different K_{Id} levels. Measuring the slope in Fig. 4(a), one can obtain the activation energy $\Delta G_f = 1.02$ ev. Figure 3(a) shows that, with decreasing temperature and increasing loading rate, K_{Id} values tend to a constant value at the lower-shelf region. This value is not related to temperature and loading rate and can be defined as an athermal activation component, K_{Idn}, which is 38.6 MPa $m^{1/2}$ by measurement from Fig. 3(a). In the transition region, the part relative to temperature and loading rate in K_{Id} values can be defined as a thermal activation component, marked as K_{Ida}. Then, the total dynamic fracture toughness, K_{Id}, can be expressed as

$$K_{Id} = K_{Idn} + K_{Ida} \qquad \text{(Eq 8)}$$

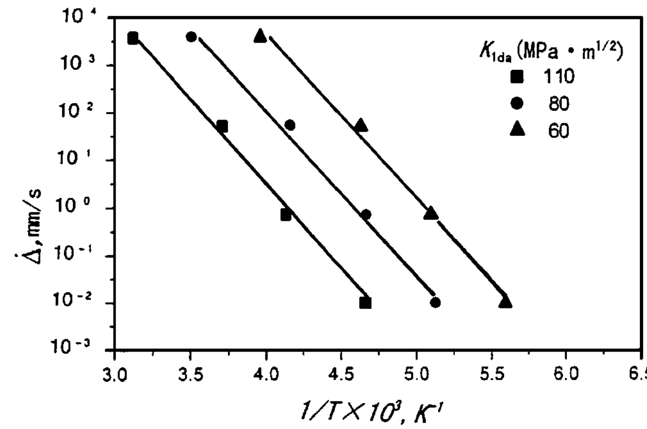

(**a**)

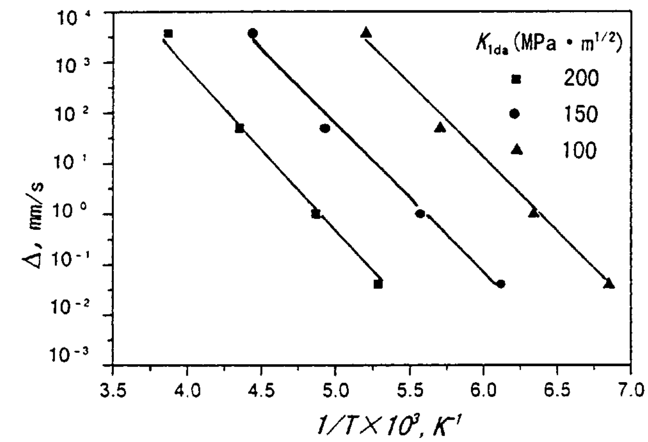

(**b**)

Fig. 4 Relations between $\dot{\Delta}$ and T^{-1} at the different K_{Id} values: (**a**) HG785C steel and (**b**) 13Ni3CrMoV steel

Because $ln\ X$ is the intercept of the lines, Fig. 4 also indicates that $ln\ X$ decreases with the increase of K_{Ida}. Hence, we presume that there is an index relationship between K_{Ida} and $ln\ X$; for example,

$$ln\ X = X_0(K_{Ida}/K_{Ido})^m \qquad \text{(Eq 9)}$$

where X_0 and m are two material parameters independent of fracture toughness and K_{Ido} is a unit fracture toughness. Taking the logarithm for Eq 9, one can obtain

$$ln\ ln\ X = ln\ X_0 + m\ ln\ (K_{Ida}/K_{Ido}) \qquad \text{(Eq 10)}$$

Figure 5 is a plot of $ln\ ln\ X$ and $ln\ (K_{Ida}/K_{Ido})$ by data from Fig. 4(a). As a good linear relation between $ln\ ln\ X$ and $ln\ (K_{Ida}/K_{Ido})$ is shown, the correctness of the assumption of Eq 9 is also verified. Measuring the slope and intercept of the line in Fig. 5 gives $m = -0.32$ and $X_0 = 215$. From Eq 9 and 7, one can obtain

$$K_{Ida} = K_{Ido}\left[\frac{1}{X_0}\left(\ln \dot{\Delta} + \frac{\Delta G_f}{k \cdot T}\right)\right]^{1/m} \qquad \text{(Eq 11)}$$

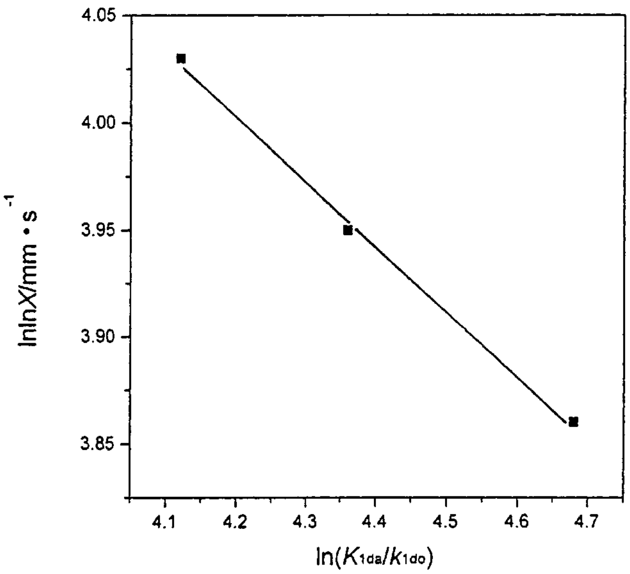

Fig. 5 Relations between ln ln X and ln (K_{1da}/K_{1do}) for HQ785C steel

Therefore, the total dynamic fracture toughness K_{Id} can be expressed as

$$K_{Id} = K_{Idn} + K_{Ido}\left[\frac{1}{X_0}\left(\ln\dot{\Delta} + \frac{\Delta G_f}{k\cdot T}\right)\right]^{1/m} \quad \text{(Eq 12)}$$

The K_{Id} values calculated by Eq 12 at different loading rates and temperatures are indicated by the dotted lines in Fig. 3(a). They are in good agreement with the experimental results. Hence, Eq 12 quantitatively describes the relationship between the dynamic fracture toughness, temperature, and loading rate for HQ785C steel.

The experimental values of the dynamic fracture toughness of 13Ni3CrMoV steel at different temperatures and loading rates were reported in Ref 8. Those test results were analyzed by using the above method. Figure 4(b) shows the linear relationship between $ln\ \dot{\Delta}$ and T^{-1} at different K_{Id} values of 13Ni3CrMoV steel. Measuring the slope gives the activation energy $\Delta\ G_f = 0.45$ ev, and measuring the values in the lower-shelf region in Fig. 3(b) gives the athermal activation component $K_{Idn} = 49.2$ MPa $m^{1/2}$. Regressing the measured $ln\ X$ values and corresponding K_{Ida} values in Fig. 4(b) gives the material parameters $m = -0.43$ and $X_0 = 292$. Then, substituting these material parameters into Eq 12 and calculating K_{Id} values from Eq 12 with different temperatures and loading rates (dotted lines in Fig. 3b), one can find that the experimental data are also in approximate agreement with the K_{Id} values calculated. This also indicates that dynamic fracture toughness is controlled by the thermal activation of dislocations under a certain range of temperatures and strain rates.

4. Discussion

In the brittle-to-ductile transition region, dynamic fracture toughness of high-strength low-alloy K_{Id} values can be divided into two parts. One part is a thermal component in K_{Id} related to the combined effect of temperature and strain rate. The second part is an athermal component in K_{Id} independent of temperature and strain rate, which is determined by the linear elastic fracture toughness controlled by effective surface energy density.[9] When the temperature is reduced to a certain critical value under some loading rate, the thermal activation process of material deformation is restrained, so that it is difficult for dislocations to move away from the crack tip. Thus, the crack can only extend along the direction of the maximum principal stress on the plane with the maximum strain energy density, resulting in brittle fracture. With the increase of temperature, the crystal lattice resistance for dislocation to move, *i.e.*, P-N force, and the resistance of point imperfections against dislocation sources decrease, so that plastic deformation easily occurs, but dislocations still need thermal activation energy to overcome barriers.[10] The higher is the loading rate, the shorter the time for dislocations to overcome the barriers by thermal activation. Therefore, dynamic fracture toughness rises with increasing temperature and decreasing loading rate. When temperature increases to a certain critical value at some loading rate, *i.e.*, the so-called upper-shelf region, the probability of dislocations being activated increases, and dislocations have sufficient time to complete thermally activated processes, so that dynamic fracture toughness becomes insensitive to temperature and loading rate.

5. Conclusions

- The ranges of K_{Id} values of high-strength low-alloy steels under different temperatures and strain rates can be divided into three regions, *i.e.*, upper-shelf region, thermal activation region, and athermal activation region.
- In the thermal activation region, with the increase of temperature and decrease of loading rate, dynamic fracture toughness rises and may be quantitatively expressed as follows:

$$K_{Id} = K_{Idn} + K_{Ido}\left[\frac{1}{X_0}\left(\ln\dot{\Delta} + \frac{\Delta G_f}{k\cdot T}\right)\right]^{1/m}$$

Acknowledgments

The authors thank D.G. Wang and Q.T. Wu, Department of Physical Metallurgy, Central Iron & Steel Research Institute, for their assistance in performing the tests. The financial support of the China Natural Science Foundation is also gratefully acknowledged.

References

1. R.W. Hertzberg: *Deformation and Fracture Mechanics of Engineering Materials,* Wiley, New York, NY, 1976.
2. L.W. Sheng and Y. Mei: *Eng. Fract. Mech.,* 1996, vol. 53 (4), pp. 633-43.
3. National Bureau Standards: GB4161-84, “Standard Test Method for Plane Strain Fracture Toughness of Metallic Materials”; GB2650-89, “Standard Impact Test Method of Metallic Materials,” National Standards of the People’s Republic of China (in Chinese).

4. J.R. Rice, P.C. Paris, and J.G. Merkle: *Progress in Flaw Growth and Fracture Toughness Testing,* ASTM STP536, Philadelphia, PA, 1973, pp. 231-45.
5. J.G. Radone and D.J. Ruben: *High Temp. Technol.,* 1994, vol. 15 (2), pp. 216-28.
6. J.L. Bassani: in *Advanced in Aerospace Structures and Materials,* S.S. Wang and W.J. Penten, eds., ASME, New York, NY, 1981.
7. C. Chi, C.Q. Gong, and W.R. Zhi: *Engineering Fracture Mechanics,* National Defense Industry Press, Beijing, 1977, pp. 275-76.
8. G.X. He: Ph.D. Thesis, Tsinghua University, 1991 (in Chinese).
9. L.W. Sheng and S. Yan: *Int. J. Fract.,* 1997, vol. 83 (4), pp. L17-L23.
10. H.J. Frost and M.F. Ashby: *Deformation Mechanism Maps,* Pergamon Press, Oxford, United Kingdom, 1982.